DRUG DESIGN OF MEDICINAL PLANTS AS A TREATMENT OF OMICRON VARIANT (COVID-19 VARIANT B.1.1.529)

FATEMEH MOLLAAMIN [1], SARA SHAHRIARI [2] AND MAJID MONAJJEMI [3]*

[1]*Department of Biomedical Engineering, Faculty of Engineering and Architecture, Kastamonu University, Kastamonu, Turkey.*
[2]*Department of Chemistry, Central Tehran Branch, Islamic Azad University, Tehran, Iran.*
[3]*Department of Chemical engineering, Central Tehran Branch, Islamic Azad University, Tehran, Iran.*

ABSTRACT

The aim of this work was identifying the physico-chemical properties of some medicinal plants which are applied in front of the Omicron Variant (Covid-19 variant B.1.1.529) symptoms. In this paper, seven medicinal ingredients for the most frequently symptoms of Omicron disease containing cough, sore throat, fever, short-breath, anorexia, muscle-joint pain, headache and Nausea-vomiting related to the fidelity level index has been run. In fact, coronaviruses (CoVs) is able to infect people and multiple types of animals through enteric, respiratory, and central nervous system maladied with considerable agents for designing anti- Omicron conjunction. In this investigation, it has been discussed the compounds of thymol, gingerol, salvinorina A, cynnamil, curcumin, pulegone and rosmarinic acid as a probable anti pandemic Omicron receptor derived from medicinal plants and herbs of thyme, ginger, salvia divinorum, cinnamon leaves, curcuma longa (turmeric), mentha pulegium (pennyroyal) and rosemary, respectively.

Anti-Omicron through the H-bonding employing the physical and chemical characteristics containing heat of formation, Gibbs free energy, electronic energy, charge distribution of active parts in the hydrogen bonding, NMR estimation of medicinal ingredients jointed to the database amino acids fragment of Tyr-Met-His as the selective zone of the Omicron, positive frequency and intensity of different normal modes of these structures have been measured. On the other hand, the simulated computations were accomplished at different steps of theory to get the more real equilibrium geometrical coordination, and IR spectral data for each of the complex proposed drugs of N-terminal or O-terminal auto-cleavage substrate were individually identified to represent the structural flexibility and substrate binding of these natural plants embedded to active site of Omicron molecule. Finally, a comparison of these structures with two configurations prepares new outlooks for modeling the substrate-based anti-targeting Omicron. This issue exhibits a feasible model for simulating a wide-spectrum of anti- Omicron medications. The structure-based optimization of these molecules has resulted two more efficacious lead materials, nitrogen and oxygen elements through producing the hydrogen bonding (H-bonding) with a rich anti- Omicron Variant (Covid-19 variant B.1.1.529).

Keywords: Omicron Variant, thymol, gingerol, salvinorina A, cynnamil, curcumin, pulegone, rosmarinic acid.

INTRODUCTION

It has been observed and evaluated the SARS-CoV-2 variant: B.1.1.529 by experts of the technical advisory group on SARS-CoV-2 Virus Evolution in 2021. The epidemiological situation in South Africa has been identified by three different peaks in announced cases, the latest of which was predominantly the Delta variant. Then, infections have increased sharply, simultaneously with finding B.1.1.529 variant.

This agent has a grand number of mutations, some of which are worrying. There is an increased risk of reinfection with this variant comparing to other VOCs. So, current SARS-CoV-2 PCR diagnostics can find this variant. Some experiments have shown that for one large PCR test, one of the three target genes is not found and this test can be applied as a sign for this variant, waiting sequencing approval. By this method, this variant has been found at more rapid amounts than previous waves in infection, recommending that this variant might have a growth privilege.

It has been proved that a detrimental change in COVID-19 epidemiology should be determined as a VOC, and the WHO has determined Omicron Variant (B.1.1.529 as a VOC).

The human is reminded to take measures to decrease their risk of COVID-19 consisting of public health and social measures such as wearing masks, hand hygiene, physical distancing, increasing ventilation of inside spaces, preventing crowded spaces, and getting vaccinated issue [1-3].

In fact, CoV closely corresponds to intense breathing syndrome CoV (SARS-CoV) which is an epidemic with short period at its living time. SARS-CoV and MERS-CoV relate to the family Coronaviridae's family as enveloped, positive stranded RNA viruses with around 30,000 nucleotides. It has been reported that the global outbreak of a life-threatening typical pneumonia caused about 800 deaths which was world identified as the harsh syndrome CoV (SARS-CoV) [4-8].

Moreover, developed investigations have indicated that the origin of SARS-CoV based on the phylogenic analysis is mostly likely from bats which are transferred to human aerosols due to intermediate hosts like infectious palm civets by the virus molecule [9-11].

So, the animal disease of CoV due to its power of intermediate transition into persons is a threat which has been summarized with the novel MERS-CoV suggesting bats and dromedary camels as the storage for this virus [12-17]. Besides, MERS-CoV declares SARS-like symptoms due to human infections including malaise, rigors, fatigues and high fevers, signs like influenza, but it has been seen later developement to a typical pneumonia in most states [18].

In some verdicts, it has been explored that a prototype of the Coronaviridae family is an infectious bronchitis virus (IBV) which relates to the genetic group III of CoV, and causes severe economic defeat for the poultry industry in the world [19-22]. Actually, the scientists have not discovered any vaccine or specific antiviral treatment ,by management concerning care of symptoms, supportive treatment, and experimental data [23].The results have shown the sample between 1% to 3% [24,25].

The elements in environment can greatly affect the secretion of secondary metabolites from tropical plants. Therefore, great attention has been paid to the secondary metabolites secreted by plants in tropical regions that may be developed as medicines [26, 27]. Several compounds, such as flavonoids, from medicinal plants, have been reported to have antiviral bioactivities [28-30]. In the present study, we investigated thymol, gingerol, salvinorina A, cynnamil, curcumin, pulegone and rosmarinic acid as the probable anti- Omicron receptor derived from medicinal plants and herbs including thyme, ginger, salvia divinorum, cinnamon leaves, curcuma longa (turmeric), mentha pulegium (pennyroyal) and rosemary (Table 1).

**Corresponding author email: smollaamin@gmail.com*

Table 1. Medicinal ingredients of thymol, gingerol, salvinorina A, cynnamil, curcumin, pulegone and rosmarinic acid as the probable anti - Omicron receptor derived from medicinal plants and herbs including thyme, ginger, salvia divinorum, cinnamon leaves, curcuma longa (turmeric), mentha pulegium (pennyroyal) and rosemary.

Medicinal species	Main ingredient	Molecular structure	Symptoms[31]
Thyme	Thymol	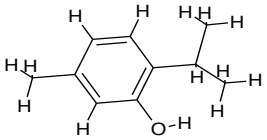	Fever
Ginger	Gingerol	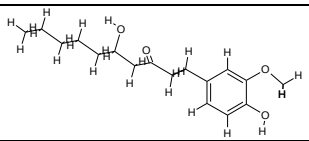	Cough
Salvia divinorum	Salvinorina A	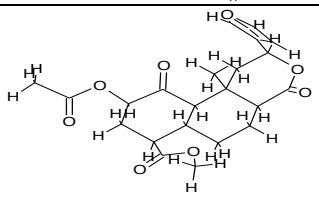	Sore throat Shortness of breath
Cinnamon leaves	Cynnamil	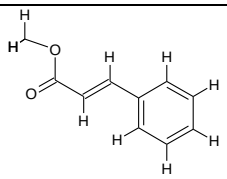	Anorexia Skin rash
Curcuma longa (turmeric)	curcumin	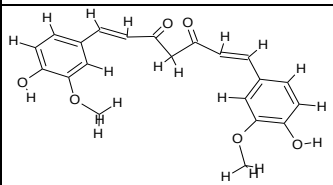	Muscle-joint pain
Mentha pulegium (pennyroyal)	Pulegone	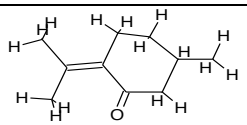	Nausea-vomiting Headache
Rosemary	Rosmarinic acid	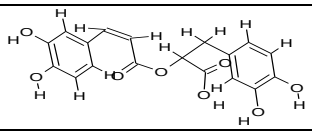	

The investigations of the present study will provide other researchers with opportunities to identify the right drug to combat Omicron (Covid-19 variant B.1.1.529) using theoretical methods to estimate the impact of hydrogen bonding in different linkage through seven medicinal plants of thymol, gingerol, salvinorina A, cynnamil, curcumin, pulegone and rosmarinic acid jointed to the active site of Omicron protein structure (Figure 1).

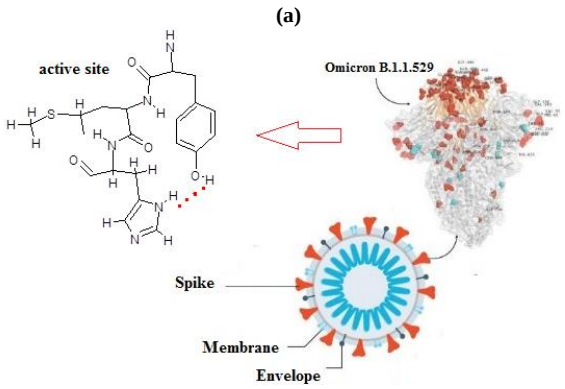

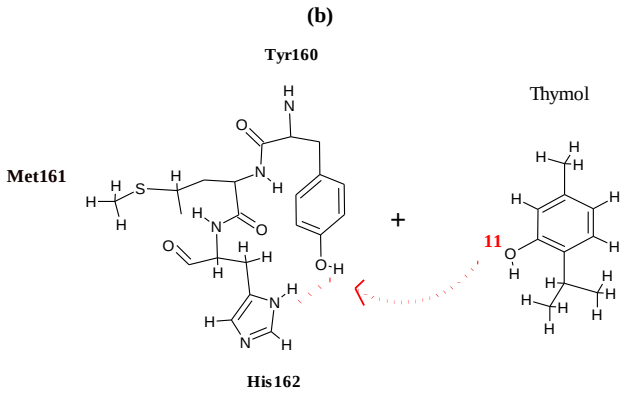

Figure 1. a) Omicron protein and its active site. **b)** The junction of thymol to TMH (Tyr160-Met161-His162) by hydrogen bonding.

MATERIAL AND METHOD

The linkage of thymol, gingerol, salvinorina A, cynnamil acetate, curcumin, pulegone and rosmarinic acid to Tyr160-Met161-His162 (TMH) active site of Omicron Variant has been accomplished in this work by forming relatively stable complexes through the hydrogen bonding. Thus, a series of quantum theoretical methods of m062x/cc-pvdz pseudo=CEP for complexes of seven inhibitors for Omicron Variant has been done due to finding the optimized coordination of the best structures of medicinal plant-Tyr160-Met161-His162 drug design model with infrared computations using the Gaussian09 program package [32].

It has been exhibited that polarization functions into the applied basis set in the computation always introduce us an important achievement on the modeling and simulation theoretical levels. Normal mode accomplishment is the verdict of harmonic potential wells by analytic methods which maintain the motion of all atoms at the same time in the vibration time scale leading to a natural explanation of molecular vibrations [33-38]. Therefore, the optimized geometry coordination of medicinal ingredients-TMH complexes toward the drug design has been run through the active site of indicated oxygen, nitrogen and hydrogen atoms in the junction of bond and torsion angles (Table 2, Figure1a,b).

Table 2. Optimized geometry coordination with m062x/cc-pvdz pseudo=CEP pseudo=CEP for thymol, gingerol, salvinorina A, cynnamil acetate, curcumin, pulegone and rosmarinic acid jointed to TMH Omicron active site through the drug design method.

INH-Omicron active site	Bond length	(Å)	Bond/Torsion angle	(º)
Thymol-TMH	N73-H 74	1.034	N73- H74-O11	175.099
	H74-O11	0.9965		
	O11-C4	1.3719	N73-H74-O11-C4	-168.336
Gingerol -TMH	N95-H 96	1.0334	N95-H96-O17	178.002
	H96-O17	0.9968		
	O17-C11	1.4062	N95-H 96-O17-C11	-128.613
Salvinorina A-TMH	N105-H106	1.0361	N105-H106-O4	178.666
	H106-O4	0.9980		
	O4-C2	1.4127	N105-H106-O4-C2	99.4304
Cinnamyl acetate-TMH	N71-H72	1.0372	N71-H72-O10	177.855
	H72-O10	0.9976		
	O10-C9	1.4223	N71-H72- O10-C9	139.376
Curcumin - TMH	N96-H97	1.0364	N96-H97-O23	178.496
	H97-O23	0.9970		
	O23-C9	1.4183	N96-H97-O23-C9	110.091
Pulegone - TMH	N49-H50	1.0350	N49-H50-O72	176.665
	H50-O72	0.9974		
	O72-C57	1.4101	N49-H50-O72-C57	172.369
Rosmarinic acid - TMH	N91-H92	1.0357	N91-H92-O6	174.51
	H92-O6	0.9968		
	O6-C5	1.406	N91-H92-O6-C5	-176.792

So, for accomplishing a stable structure of medicinal plant linkage of Omicron active site, geometry optimization plus the NMR estimation, the frequency and intensity of the vibrational modes were calculated with the quantum mechanical method, and the principal vibrational modes were analyzed by their changes of Gibbs free energy at 300K of temperature.

Moreover, the data has been achieved from thermodynamic parameters of ΔG, ΔH and ΔS for medicinal plant - Omicron drug design. Thermochemistry analysis follows the frequency and normal mode data. The zero-point energy output in Gaussian-09 has been expanded and corrected as: Thermal correction to energy, thermal correction to enthalpy and thermal correction to the Gibbs free. In addition the total energies can be calculated as sum of electronic and zero point energies, sum of electronic and thermal energies, sum of electronic and thermal enthalpies and sum of electronic and thermal Gibbs free energies values.

The computational data was done at various levels of theory to gain the more accurate equilibrium geometrical results and IR spectral data for each of the identified compounds. It is supposed that an additional diffuse and polarization functions into the basis set applied in the computation conduct us to the magnificent progress on the results of theoretical computations.

The method of simulation exhiits the approaches which produce a common template of a model at a special temperature by computing all physicochemical properties among the partition function parameter [34].

Therefore, every part of the systems including medicinal ingredients-TMH has been optimized using ab-inito via density functional theory including ECP calculations with pseudo=CEP basis sets. In addition, those systems have been evaluated via QM/MM approach through an ONIOM method. In our study, differences of force fields are debated through comparing density and energies with OPLS and AMBER via Monte Carlo optimization. In addition, a Hyperchem professional release 7.01 program has been applied for some additional keywords such as PM3MM, PM6 and pseudo=CEP [39, 40].

So, the Polarizable Continuum Model, PCM, is the most popular SCRF model based on apparent surface charges expanding to discuss non-electrostatic impacts using scaled point theory [41, 42].

Rinaldi and Rivail developed the most common levels of the SCRF method of multiple expansions with an algorithm based on the use of a strict multipolar expansion up to the 7th order by Frisch that is currently available at both semi-empirical and ab initio levels of theory [43-45].

Two scientists, Onsager and Kirkwood, have arranged an intention for various continuum solvation examples of a multiple expansion, MPE, of the solute charge distribution [46-48]. Then, Wiberg and co-workers improved Onsager-SCRF for the Gaussian program [49,50].

Solvation is illustrated in terms of a dipole moment with an iterative path of quantum mechanics calculations on the structure. The perspective of Onsager-SCRF was one to directly apply almost all of the computational characteristics of Gaussian program. The dielectric continuum models like the self-consistent reaction field approach are efficient in applying account the long range of solute-solvent electrostatic interactions and the effect of solvent polarization. Another theoretical level is combination of molecular mechanics (MM) solvent molecule with quantum mechanics level (QM) for electronic structure of the solute molecule named QM/MM which can modify deficiency of the dielectric continuum model of theory [51,52].

RESULTS AND DISCUSSION

The theoretical calculations of nuclear magnetic resonance on the database of amino acids in beta sheet conformation of Tyr160-Met161-His162 and the main ingredients of medicinal plants including salvinorina A, cynnamil acetate, curcumin**,** pulegone and rosmarinic acid have been estimated to unravel the indicated atoms of H,N,O in the active sites of these anti-virus drugs through the formation of hydrogen bonding by indicating the attack zone of TMH residues (Figure2a-f).

(a)

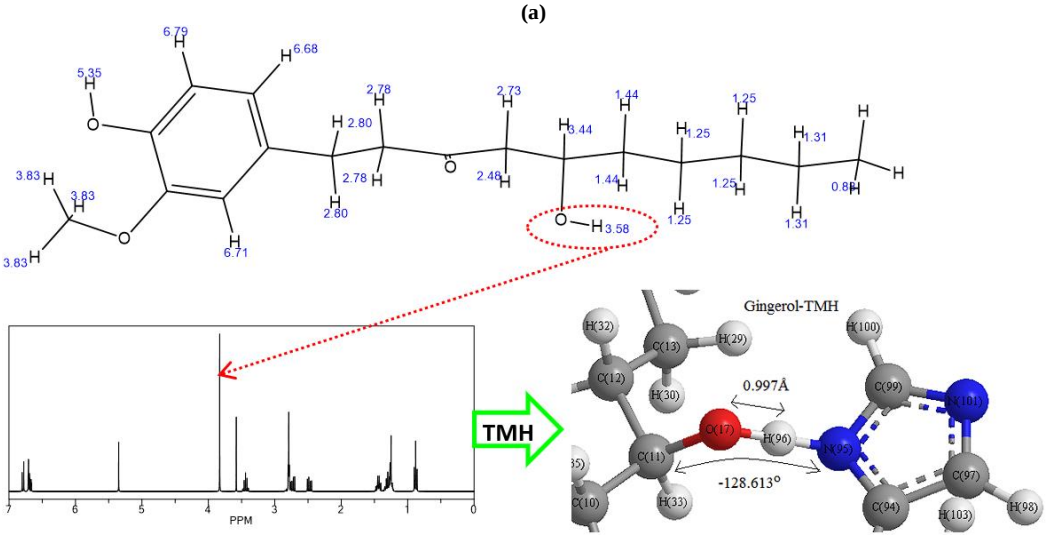

(b)

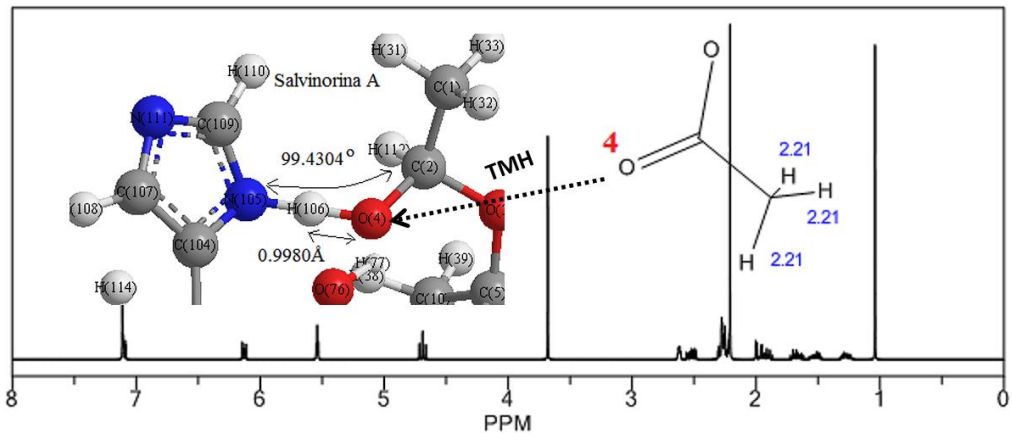

(c)

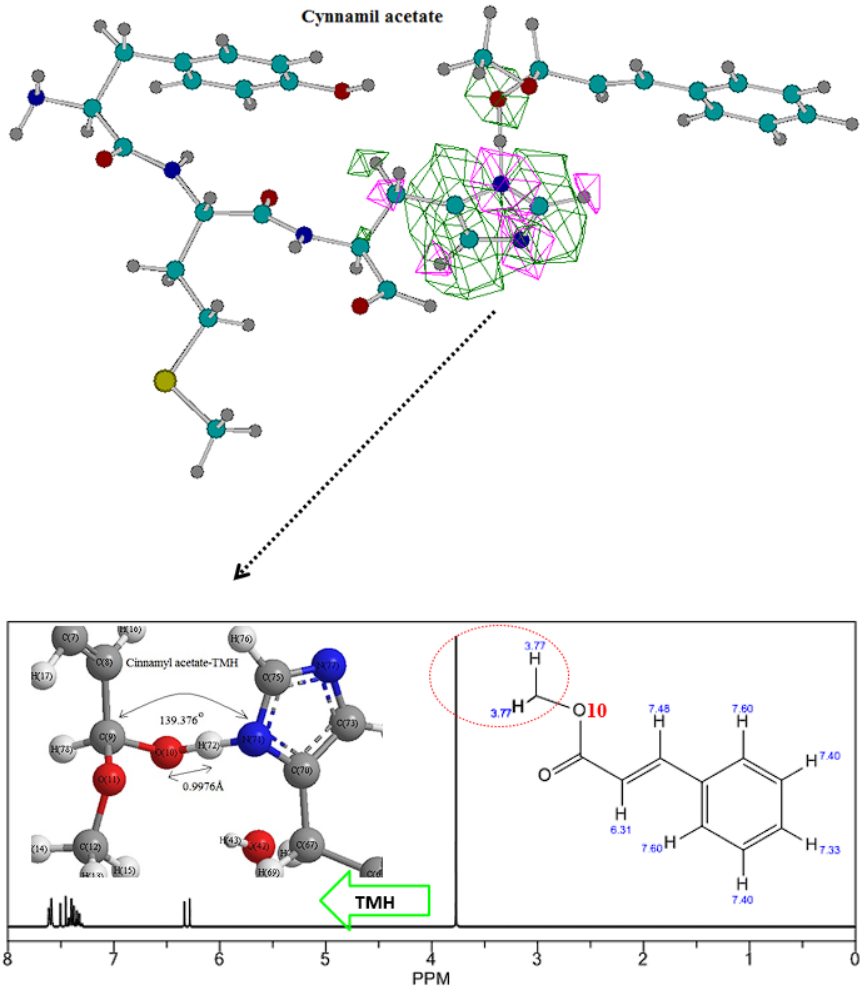
Cynnamil acetate
Cinnamyl acetate-TMH
139.376°
0.9976Å
TMH
PPM

(d)

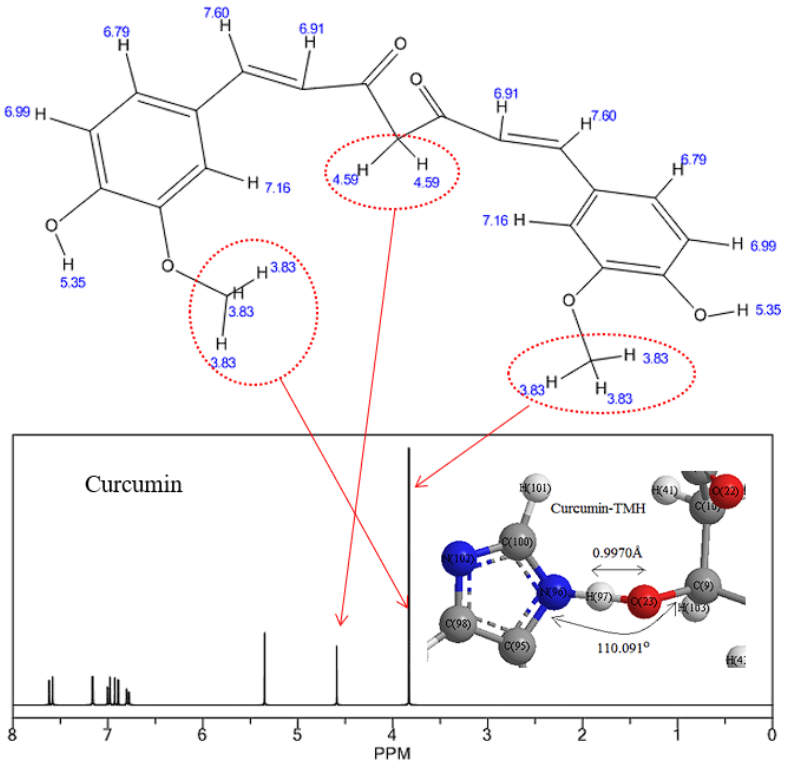
Curcumin
Curcumin-TMH
0.9970Å
110.091°
PPM

(e)

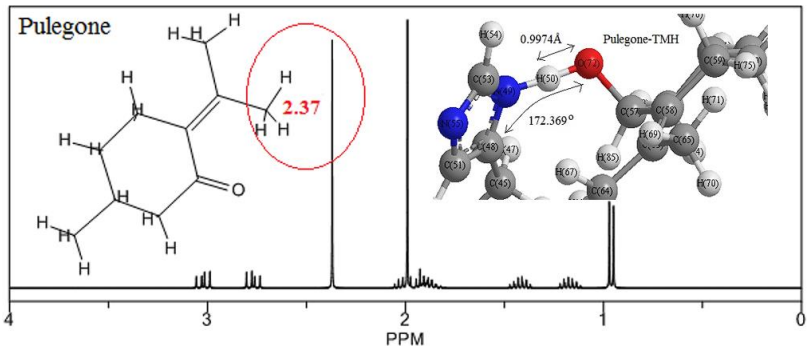

(f)

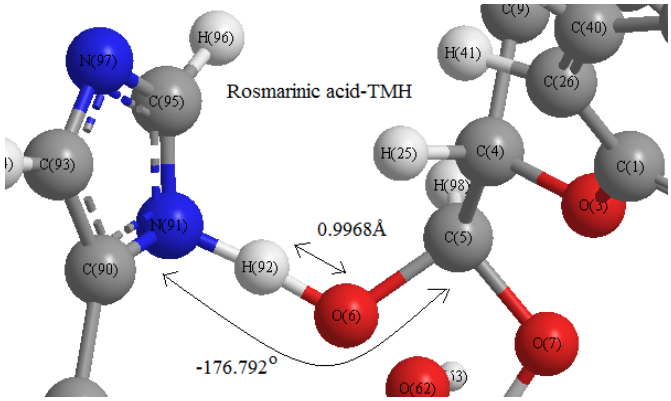

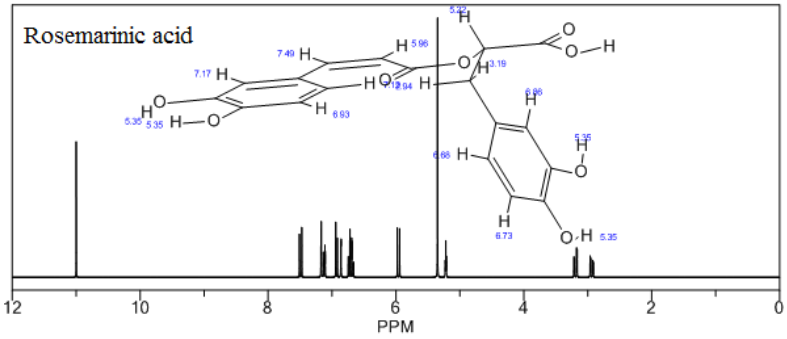

Figure 2. The results of NMR spectra of **a)** gingerol **b)** salvinorina A **c)** cynnamil acetate **d)** curcumin **e)** pulegone **f)** rosmarinic acid jointed to TMH Omicron active site through the drug design method by indicating the active zone of TMH in the drug design process.

The amounts of NMR calculation introduce the active sites of main ingredients of medicinal species for linking to the Tyr160-Met161-His162 (TMH) in forming the anti-virus drugs while each active atom of oxygen and nitrogen as the electronegative atoms for attaching to the hydrogen denotes the maximal shift in all levels in the NMR spectra (Figure 2a-f).

Then two main ingredients of medicinal plants including thymol and gingerol have been computed for stabilizing the junction of Tyr160-Met161-His162 as the anti-Omicron Variant through the drug design method using IR spectroscopy using Gaussian09 program package (Figure 3 a,b).

(a)

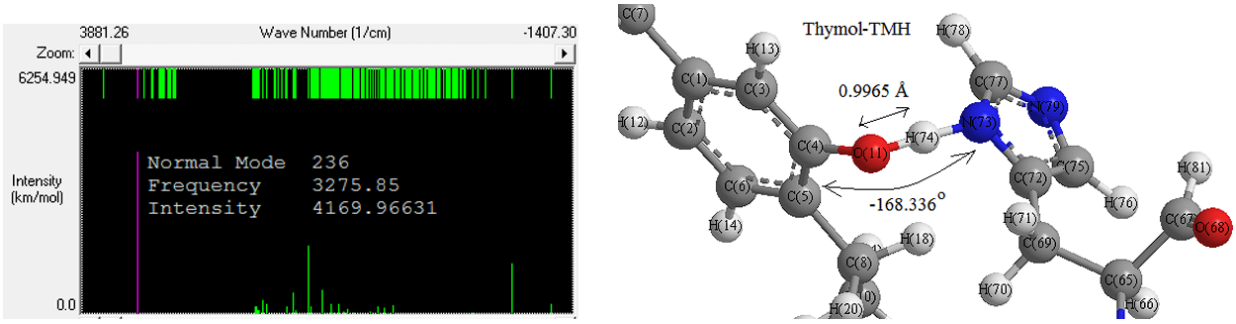

(b)

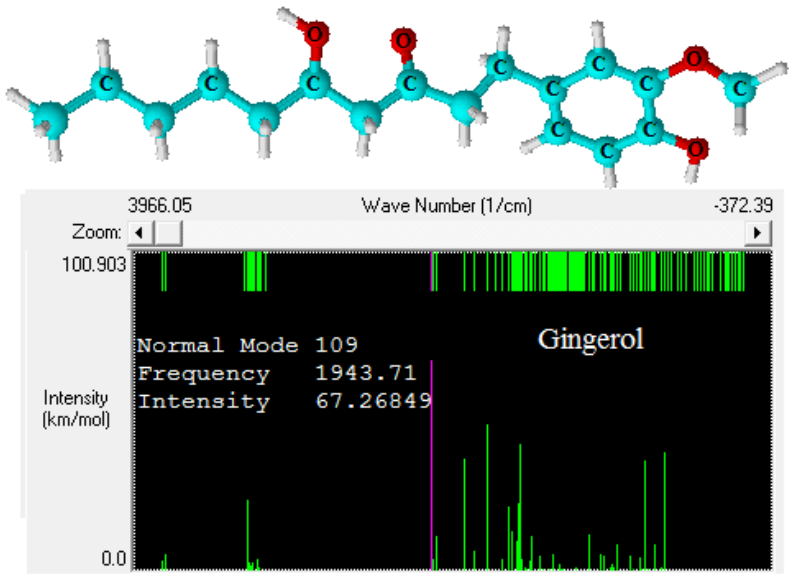

Figure 3. IR spectrum of **a)** thymol and **b)** gingerol jointed to TMH through the drug design method calculated by m062x/cc-pvdz pseudo=CEP.

So, the thermodynamic characteristics of ΔG, ΔS, Electronic Energy and Core-Core interaction have determined the stable anti-Omicron Variant complexes of main ingredients of medicinal species-TMH through the H-bonding formation using the drug design approach (Table3 and Figure4).

Table 3. Physical and Thermochemical properties of thymol, gingerol, salvinorina A, cynnamil acetate, curcumin, pulegone and rosmarinic acid jointed to Omicron active site (TMH) complexes at 300 K.

Main ingredient - Omicron active site	ΔG ×10^{-4} (kcal/mol)	ΔS (kcal/K.mol)	$E_{electronic}$×10^{-4} (kcal/mol)	$E_{core-core}$×10^{-4} (kcal/mol)
Tymol	-15.2864	509.7272	-166.9099	151.6234
Gingerol	-19.6580	655.0303	-244.8435	225.1855
Salvinorina A	-23.7959	792.74793	-330.9869	307.1910
Cynnamil acetate	-15.8876	529.8103	-167.0736	151.1860
Curcumin	-21.9310	731.6760	-267.1469	245.2159
Pulegone	-15.4311	514.4416	-175.3951	159.9640
rosmarinic acid	-22.3452	744.4824	-268.8752	246.5299

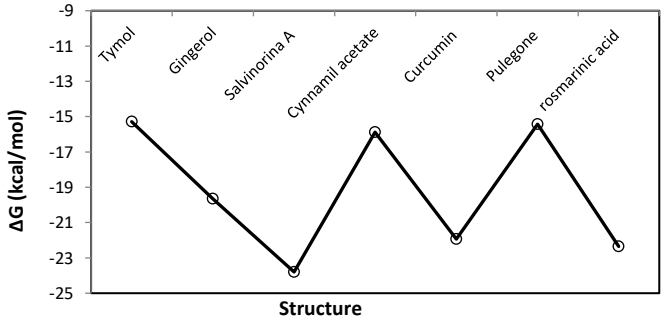

Figure 4. Changes of ΔG for the stable anti-Omicron Variant complexes of thymol, gingerol, salvinorina A, cynnamil acetate, curcumin, pulegone and rosmarinic acid jointed to TMH through the H-bonding formation using the drug design method.

As a matter of fact, the difference of ΔH_F among thymol, gingerol, salvinorina A, cynnamil acetate, curcumin, pulegone and rosmarinic acid jointed to Omicron has been discussed the H-bonding due to the database of amino acids in beta sheet conformation; Tyr160-Met161-His162 as the active site of the COVID-19 variant B.1.1.529 molecule (Table 4, Figure5).

Table 4. The Heat of formation, ΔH_F (kcal/mol), among thymol, gingerol, salvinorina A, cynnamil acetate, curcumin, pulegone and rosmarinic acid jointed to Omicron active site (TMH) complexes at 300 K.

ΔH_{TMH}×10^{-4} 25.8242 (kcal/mol)	ΔH_{Thymol}	$\Delta H_{(Thymol\text{-}TMH)}$	ΔH_F×10^{-4} =$\Delta H_{(Thymol\text{-}TMH)}$ – (ΔH_{TMH} +ΔH_{Thymol})
	-28.9166	53.7594	-25.8160
	$\Delta H_{Gingerol}$	$\Delta H_{(gingerol\text{-}TMH)}$	ΔH_F ×10^{-4} =$\Delta H_{(gingerol\text{-}TMH)}$ – (ΔH_{TMH} +$\Delta H_{gingerol}$)
	-145.3195	-70.9553	-25.8168
	$\Delta H_{Salvinorina\ A}$	$\Delta H_{(Salvinorina\ A\text{-}TMH)}$	ΔH_F×10^{-4} = $\Delta H_{(Salvinorina\ A\text{-}TMH)}$ – (ΔH_{TMH} +$\Delta H_{Salvinorina\ A}$)
	-218.2009	-134.8384	-25.8159
	$\Delta H_{Cynnamil\ acetate}$	$\Delta H_{(Cynnamil\ acetate\text{-}TMH)}$	ΔH_F ×10^{-4} =$\Delta H_{(Cynnamil\ acetate\text{-}TMH)}$ – (ΔH_{TMH} +$\Delta H_{Cynnamil\ acetate}$)
	-29.6736	66.9460	-25.8146
	$\Delta H_{Curcumin}$ 115.3026	$\Delta H_{(Curcumin\text{-}TMH)}$ 192.8237	ΔH_F×10^{-4} =$\Delta H_{(Curcumin\text{-}TMH)}$ – (ΔH_{TMH} +$\Delta H_{Curcumin}$) -25.8165
	$\Delta H_{Pulegone}$ -48.9909	$\Delta H_{(Pulegone\text{-}TMH)}$ 21.7634	ΔH_F×10^{-4} = $\Delta H_{(Pulegone\text{-}TMH)}$ – (ΔH_{TMH} +$\Delta H_{Pulegone}$) -25.8172
	$\Delta H_{Rosmarinic\ acid}$ 355.7935	$\Delta H_{(Rosmarinic\ acid\text{-}TMH)}$ -107.7616	ΔH_F ×10^{-4} = $\Delta H_{(Rosmarinic\ acid\text{-}TMH)}$ – (ΔH_{TMH} +$\Delta H_{Rosmarinic\ acid}$) -25.8706

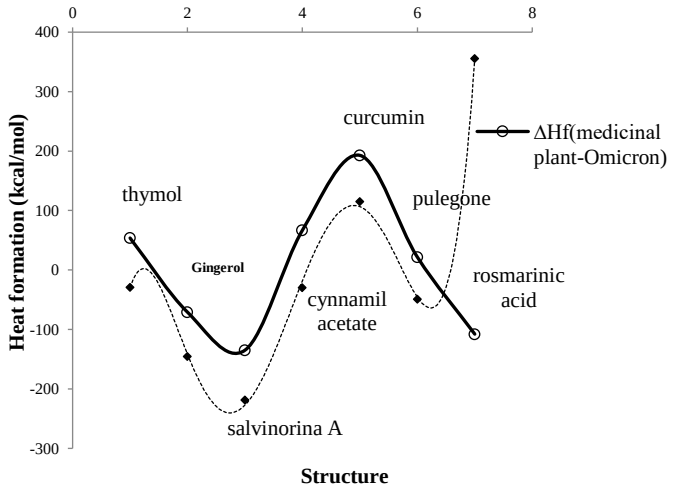

Figure 5. The difference of ΔH_F among thymol, gingerol, salvinorina A, cynnamil acetate, curcumin, pulegone and rosmarinic acid jointed to Omicron active site (TMH) complexes at 300 K.

In thymol, gingerol, cynnamil acetate, and pulegone jointed to the database of amino acids in beta sheet conformation, Tyr160-Met161-His162, as the active site of Omicron protein in the process of drug design, the frequency and intensity of various infrared normal modes of medicinal ingredients-TMH complexes have been found to be significantly different through the stability of H-bonding formed between active site of COVID-19 variant B.1.1.529 and medicinal ingredients which founds the anti-Omicron Variant (Table 5 & Figure6).

Table5. Calculated frequency and intensity of thymol, gingerol, cynnamil acetate, and pulegone as anti-Omicron drugs in different normal modes of infrared spectra.

inhibitor	Normal mode	Frequency (1/cm)	Intensity (km/mol)	Dipole (Debyes)
Thymol	236	3275.85	4169.9663	8.826
Gingerol	109	1943.71	67.268	4.291
Cynnamil acetate	234	3680.71	115.4354	5.034
Pulegone	248	3424.38	829.8741	5.439

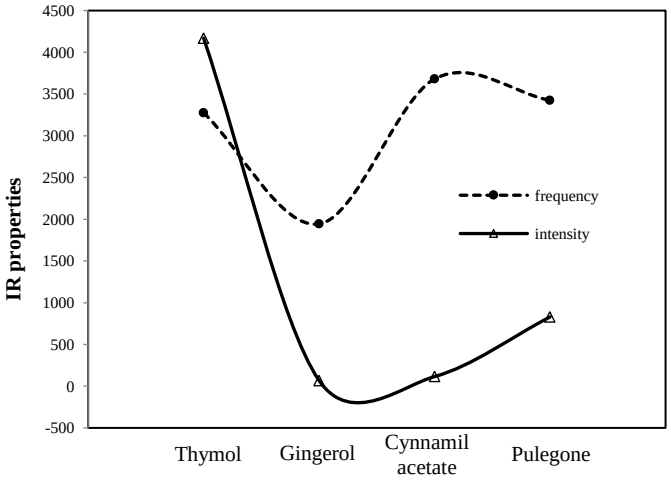

Figure 6. IR spectrum for medicinal plants of thymol, gingerol, cynnamil acetate, and pulegone as anti-Omicron drugs in different normal modes (Table 5).

The parameters of frequency and intensity TMH-junction were found to be significantly different with each medicinal ingredient treatment including thymol, gingerol, cynnamil acetate, and pulegone.

It has been observed that by increasing the activity of atoms in the active site of medicinal ingredients, the frequency and intensity of medicinal ingredients-Tyr160-Met161-His162 junction also have increased from 1943.71to 3680.711/cm and from 67.268 to 4169.9663 km/mol, respectively, with forming hydrogen bonding (Table 5 & Figure 6).

Although we have little information about the interaction of medicinal drugs with Omicron Variant, database amino acids fragment of Tyr160-Met161-His162 as the selective zone of the COVID-19 variant B.1.1.529 were found to induce frequency and intensity of spectra.

After that, the atomic charge of indicated atoms of oxygen, nitrogen and hydrogen in the junction of thymol, gingerol, salvinorina A, cynnamil acetate, curcumin, pulegone and rosmarinic acid with Tyr160-Met161-His162 have been evaluated in the zone of H-bonding formation (Table 6).

Table 6. The values of atomic charge for labeled oxygen atoms in the attachment of thymol, gingerol, salvinorina A, cynnamil acetate, curcumin, pulegone and rosmarinic acid with Tyr160-Met161-His162.

Thymol	**charge**	**Gingerol**	**charge**	**Salvinorina A**	**charge**
O11	-0.2600	O17	-0.3116	O3	-0.2000
		O18	-0.3030	O4	-0.3842
		O19	-0.1741	O12	-0.2334
Pulegone	**charge**	O20	-0.2315	O13	-0.3639
O17	-0.3401			O20	-0.2976
				O22	-0.2428
				O25	-0.3373
				O28	-0.0394
Cynnamil acetate	**charge**	**Curcumin**	**charge**	**Rosmarinic acid**	**charge**
O10	-0.3909	O20	-0.1938	O2	0.1443
O11	-0.2390	O21	-0.2384	O3	-0.2044
		O22	-0.3473	O6	-0.3777
		O23	-0.3482	O7	-0.2784
		O24	-0.2328	O16	-0.2302
		O25	-0.2122	O17	-0.2473
				O33	-0.2279
				O34	-0.2227

In Figure 7, it has been plotted the changes of atomic charge for labeled oxygen atoms through optimized thymol, gingerol, salvinorina A, cynnamil acetate, curcumin, pulegone and rosmarinic acid with Tyr160-Met161-His162 complexes due to formation of H-bonding; so, the results of table 6 in a polar zone have declared the stability of Omicron Variant drugs which have been modeled using the drug design method.

The biggest fluctuation in Figure 7 has been seen for the sample of salvinorina A - Tyr160-Met161-His162 considering the oxygen as the electronegative atoms in formation the H-bonding through using the drug design method which has suggested the modeling of anti-Omicron Variant.

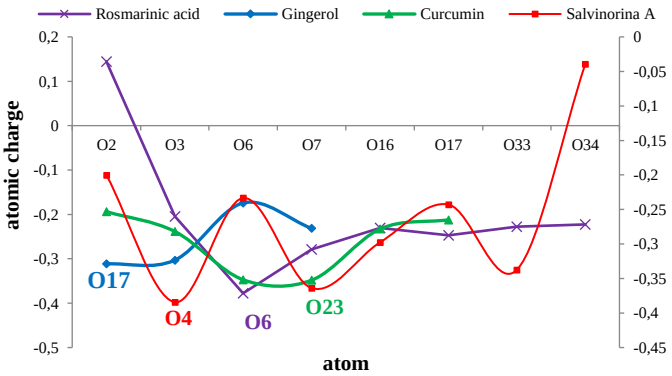

Figure7. Comparison of atomic charge versus labeled of oxygen atoms in the junction of active sites of thymol, gingerol, salvinorina A, cynnamil acetate, curcumin, pulegone and rosmarinic acid with Tyr160-Met161-His162.

In fact, the perspective of Figure 7 has proposed the reason for existing observed various results of the atomic charge on medicinal plant-Omicron variant complexes as the anti- COVID-19 variant B.1.1.529 which are principally related to the position of active cites of indicated oxygen, nitrogen and hydrogen atoms in the junction of bond angles. In fact, the spin density and partial charges have been obtained by fitting the electrostatic potential to fix the charge of oxygen and nitrogen with high electronegativity in junction of electrophilic group of hydrogen in the structures of medicinal plant-Omicron variant as the anti-virus drugs which conduct us toward the industry of drug design.

CONCLUSION

Natural drugs of thymol, gingerol, salvinorina A, cynnamil acetate, curcumin, pulegone and rosmarinic acid are capable to join the database amino acids fragment of Tyr160-Met161-His162 as the selective zone of the Omicron Variant (COVID-19 variant B.1.1.529) through indicating the shift in their frequency and intensity spectra after estimation by NMR method which are affected by the atomic configuration of the anti-virus molecules.

In fact, the stability of H-bonding between seven medicinal ingredients of thymol, gingerol, salvinorina A, cynnamil acetate, curcumin, pulegone and rosmarinic acid and Omicron Variant (COVID-19 variant B.1.1.529) through the formation anti- Omicron Variant through two probabilities of N$\cdots$H and O$\cdots$H with different atomic charges have been investigated using IR methods. So, the thermodynamic properties of Gibbs free energy, enthalpy of formation, Electronic Energy, Core-Core interaction have approved the stability of anti-Omicron Variant due to H-bonding formation using the drug design method.

REFERENCES

1. Zhang, J.; Zhou, L.; Yang, Y.; Peng, W.; Wang, W.; Chen, X. Therapeutic and triage strategies for 2019 novel coronavirus disease in fever clinics. *Lancet* **2020**, 395, e39. https://doi.org/10.1016/S0140-6736(20)30313-5.
2. Pandey, U.; Greninger, A.L.; Levin, G.R. Pathogen or bystander: clinical significance of detecting human herpesvirus 6 in pediatric cerebrospinal fluid. *J Clin Microbiol* **2020**, *58*, e00313-e00320. https://doi.org/10.1128/JCM.00313-20.
3. Mollaamin,F.; Esmkhani,R.; Monajjemi,M. Mutations in Novel COVID-19 Make it More Dangerous: Prevention Via Scientific Approaches. *Biointerface Res. Appl. Chem***2021**, *11*(3), 10546-10558. https://doi.org/10.33263/BRIAC113.1054610558.
4. Yan, B.; Chu, H.; Yang, D.; Sze, K.-H.; Lai, P.-M.; Yuan, S.; Shuai, H.; Wang, Y.; Kao, R.Y.-T.; Chan, J.F.-W.; Yuen, K.-Y. Characterization of the Lipidomic Profile of Human Coronavirus-Infected Cells: Implications for Lipid Metabolism Remodeling upon Coronavirus Replication. *Viruses* **2019**, *11*,73. https://doi.org/10.3390/v11010073.
5. Fouchier, R. A.M.; Kuiken, T.; Schutten,M.; van Amerongen,G.; van Doornum, G.J.J.; van den Hoogen, B.G.; Peiris,M.; Lim,W.; Stohr,K.; and Osterhaus, A.D.M.E. Aetiology: Koch's postulates fulfilled for SARS virus. *Nature* **2003**, *423*,240. https://doi.org/10.1038/423240a.
6. Ksiaze k, T. G.; Erdman,D.; Goldsmith, C. S.; Zaki, S. R.; Peret,T.; Emery,S.; Tong,S.; Urbani,C.; Comer,J.A.; Lim,W.; Rollin,P.E.; Dowell, S.F.; Ling,A.E.; Humphrey, C.D.; Shieh, W.J.; Guarner,J.; Paddock,C.D.; Rota,P.; Fields,B.; DeRisi,J.; Yang, J.Y.; Cox,N.; Hughes, J.M.; LeDuc, J.W.; Bellini, W.J.; and Anderson. L.J. A novel coronavirus associated with severe acute respiratory syndrome. *N. Engl. J. Med* **2003**, *348*, 1953-1966. https://doi.org/10.1056/NEJMoa030781.
7. Shi, C.S.; Nabar, N.R.; Huang, N.N.; et al. SARS-Coronavirus Open reading frame-8b triggers intracellular stress pathways and activates NLRP3 inflammasomes. *Cell Death Discov*. **2019**;5:101. https://doi.org/10.1038/s41420-019-0181-7.
8. Mollaamin, F. Function of Anti-CoV Structure Using INH [1-6]- Tyr160-Met161-His162 Complex. *Biointerface Res. Appl. Chem* **2021**, *11*(6), 14433 - 14450. https://doi.org/10.33263/BRIAC116.1443314450.
9. Mitton, B.; Rule, R.; Said, M. Laboratory evaluation of the BioFire FilmArray Pneumonia plus panel compared to conventional methods for the identification of bacteria in lower respiratory tract specimens: a prospective cross-sectional study from South Africa. *Diagn Microbiol Infect Dis* **2021**, *99*, 115236. https://doi.org/10.1016/j.diagmicrobio.2020.115236.
10. Kao,C.-C.; Chiang,H.-T.; Chen,C.-Y.; Hung,C.-T.; Chen,Y.-C.; Su,L.-H.; Shi,Z.-Y. et al. National bundle care program implementation to reduce ventilator-associated pneumonia in intensive care units in Taiwan. *J Microbiol Immunol Infect* **2019**, *52*, 592-597. https://doi.org/10.1016/j.jmii.2017.11.001.
11. Yen, M.Y.; Schwartz, J.; Chen, S.Y.; King, C.C.; Yang, G.Y.; Hsueh, P.R. Interrupting COVID-19 transmission by implementing enhanced traffic control bundling: Implications for global prevention and control efforts. *J Microbiol Immunol Infect* **2020**, *53*,377-380. https://doi.org/10.1016/j.jmii.2020.03.011.
12. Álvarez-Lerma, F.; Sánchez García, M.; The multimodal approach for ventilator-associated pneumonia prevention-requirements for nationwide implementation. *Ann Transl Med* **2018**, 6, 420. https://doi.org/10.21037/atm.2018.08.40.
13. Caméléna, F.; Moy, A.C.; Dudoignon, E.; Poncin, T.; Deniau, B.; Guillemet, L.; Le Goff, J. et al. *Diagn Microbiol Infect Dis* **2021**, *99*, 115183. https://doi.org/10.1016/j.diagmicrobio.2020.115183.
14. Dien Bard, J.; McElvania, E. Panels and Syndromic Testing in Clinical Microbiology. *Clin Lab Med* **2020**, *40*, 393-420. https://doi.org/10.1016/j.cll.2020.08.001.
15. 15. Van, T.T.; Kim,T.H.; Butler-Wu, S.M. Evaluation of the Biofire FilmArray meningitis/encephalitis assay for the detection of Cryptococcus neoformans/gattii. *Clin Microbiol Infect* **2020**, *S1198-743X*, 30031-30038. https://doi.org/10.1016/j.cmi.2020.01.007.
16. Tansarli, G.S.; Chapin, K.C. Diagnostic test accuracy of the BioFire(R) FilmArray(R) meningitis/encephalitis panel: a systematic review and meta-analysis. *Clin Microbiol Infect* **2020**, *26*, 281-290. https://doi.org/10.1016/j.cmi.2019.11.016.
17. Nabower, A.M.; Miller, S.; Biewen,B. Association of the FilmArray meningitis/encephalitis panel with clinical management. *Hosp Pediatr*. **2019**,9,763-769. https://doi.org/10.1542/hpeds.2019-0064.
18. Cailleaux, M.; Pilmis, B.; Mizrahi, A. Impact of a multiplex PCR assay (FilmArray(R)) on the management of patients with suspected central nervous system infections. *Eur J Clin Microbiol Infect Dis* **2020**, *39*, 293-297. https://doi.org/10.1007/s10096-019-03724-7.
19. She, R.C.; Bender, J.M. Advances in rapid molecular blood culture diagnostics: healthcare impact, laboratory implications, and multiplex technologies. *J Appl Lab Med* **2019**, *3*, 617-630. https://doi.org/10.1373/jalm.2018.027409.
20. Juttukonda, L.J.; Katz, S.; Gillon, J. Impact of a rapid blood culture diagnostic test in a children's hospital depends on Gram-positive versus Gram-negative organism and day versus night shift. *J Clin Microbiol* **2020**, *58*, e01400–e01419. https://doi.org/10.1128/JCM.01400-19.
21. Bakhshi, K.; Mollaamin, F.; Monajjemi, M. Exchange and Correlation Effect of Hydrogen Chemisorption on Nano V(100) Surface: A DFT Study by Generalized Gradient Approximation (GGA). *Journal of Computational and Theoretical Nanoscience* **2011**, *8*, 763-768, https://doi.org/10.1166/jctn.2011.1750.
22. Blauwkamp, T.A.; Thair, S.; Rosen, M.J. Analytical and clinical validation of a microbial cell-free DNA sequencing test for infectious disease. *Nat Microbiol* **2019**, *4*, 663-674. https://doi.org/10.1038/s41564-018-0349-6.
23. Hagen, A.; Eichinger, A.; Meyer-Buehn, M. Comparison of antibiotic and acyclovir usage before and after the implementation of an on-site FilmArray meningitis/encephalitis panel in an academic tertiary pediatric hospital: a retrospective observational study. *BMC Pediatr* 2020,*20*, 56. https://doi.org/10.1186/s12887-020-1944-2.
24. Mollaamin, F. Function of Anti-CoV Structure Using INH [1-6]- Tyr160-Met161-His162 Complex. *Biointerface Res. Appl. Chem***2021**, *11*(6), 14433 – 14450. https://doi.org/10.33263/BRIAC116.1443314450.
25. Lee, S.H.; Ruan, S.Y.; Pan, S.C.; Lee, T.F.; Chien, J.Y.; Hsueh P.R. Performance of a multiplex PCR pneumonia panel for the identification of respiratory pathogens and the main determinants of resistance from the lower respiratory tract specimens of adult patients in intensive care units. *J Microbiol Immunol Infect* **2019**, *52*, 920-928. https://doi.org/10.1016/j.jmii.2019.10.009.
26. G. Guerriero,G. *et al*., Production of plant secondary metabolites: Examples, tips and suggestions for biotechnologists. *Genes (Basel)*. **2018**, *9*(6) 34-46. https://doi: 10.3390/genes9060309.
27. Yang, L.; Wen, K. S.; Ruan, X.; Zhao, Y.X.; Wei, F. and Wang, Q. Response of plant secondary metabolites to environmental factors, *Molecules* **2018**, *23* (4), 1-26. https://doi: 10.3390/molecules23040762.
28. Zakaryan, H.; Arabyan, E.; Oo, A.; Zandi, K. Flavonoids: promising natural compounds against viral infections. *Arch. Virol.* **2017**,*162* (9), 2539-2551. https://doi: 10.1007/s00705-017-3417-y.
29. Seema,T.M.;Thyagarajan,S.P. Pa-9: A flavonoid extracted from plectranthus amboinicus inhibits HIV-1 protease. *Int. J. Pharmacogn. Phytochem. Res.* **2016**, *8*(6), 1020-1024.
30. Jo, S.; Kim, S.; Shin, D.H., Kim,M.S. Inhibition of SARS-CoV 3CL protease by flavonoids. *J. Enzyme Inhib. Med. Chem.* **2020**, 35(1), 145-151, https://doi: 10.1080/14756366.2019.1690480.

31. Akbulut, S. Medicinal Plants Preferences for the Treatment of COVID-19 Symptoms in Central and Eastern Anatolia, Kastamonu Univ., *Journal of Forestry Faculty*, 2021, 21(3): 196-207. https://doi:10.17475/kastorman.1048372.
32. Frisch, M.J.; Trucks, G.W.; Schlegel, H.B.; Scuseria, G.E.; Robb, M.A.; Cheeseman, J.R.; Scalmani, G.; et al. *Gaussian 09, Revision B.01*. **2010**. Gaussian Inc., Wallingford.
33. Mollaamin, F.; Monajjemi, M. Harmonic Linear Combination and Normal Mode Analysis of Semiconductor Nanotubes Vibrations. *J. Comput. Theor. Nanosci* **2015**, *12*, 1030-1039. https://doi.org/10.1166/jctn.2015.3846.
34. Roy, T. K.; Kopysov, V.; Pereverzev, A.; Šebek, J.; Gerber, R. B.; Boyarkin, O. V. Intrinsic structure of pentapeptide Leu-enkephalin geometry optimization and validation by comparison of VSCF-PT2 calculations with cold ion spectroscopy. *Phys. Chem. Chem. Phys.* **2018**, *20*, 24894–24901. https://doi.org/10.1039/c8cp03989e.
35. Ni, W.; Li, G.; Zhao, J.; Cui, J.; Wang, R.; Gao, Z.; Liu, Y. Use of Monte Carlo simulation to evaluate the efficacy of tigecycline and minocycline for the treatment of pneumonia due to carbapenemase-producing Klebsiella pneumoniae. *Infect Dis (Lond)* **2018**,*50* ,507-513. https://doi.org/ 10.1080/23744235.2018.1423703.
36. Kawczak, P.; Bober, L.; Bączek, T. QSAR analysis of selected antimicrobial structures belonging to nitro-derivatives of heterocyclic compounds. *Lett Drug Des Discov* **2018c**, *17*, 214-225 https://doi.org/10.2174/1570180815666181004112947.
37. McArdle,S.;Mayorov,A.;Shan,X.;Benjamin,S.; Yuan,X. Digital quantum simulation of molecular vibrations. *Chem. Sci*. **2019**, *10*, 5725-5735. https://doi.org/10.1039/C9SC01313j.
38. Wang, S. Efficiently Calculating Anharmonic Frequencies of Molecular Vibration by Molecular Dynamics Trajectory Analysis. *ACS Omega* **2019**, *4*, 9271- 9283. https://doi: 10.1021/acsomega.8b03364.
39. Monajjemi, M.; Mollaamin, F.; Gholami, M.R.; Yoosbashizadeh, H.; Sadrnezhad, S.K.; Passdar H.Quantum chemical parameters of some organic corrosion inhibitors, pyridine, 2-picoline 4-picoline and 2,4-lutidine, adsorption at aluminum surface in hydrocholoric and nitric acids and comparison between two acidic media. *MAIN GROUP MET CHEM* **2003**, *26*, 349-361. https://doi.org/10.1515/MGMC.2003.26.6.349.
40. Khaleghian, M.; Zahmatkesh, M.; Mollaamin, F.; Monajjemi, M. Investigation of Solvent Effects on Armchair Single-Walled Carbon Nanotubes: A QM/MD Study. *Fuller. Nanotub. Carbon Nanostructures.*,**2011,** *19*, 251-261, https://doi.org/10.1080/15363831003721757.
41. Lee, V.S.; Nimmanpipug, P.; Mollaamin, F.; Kungwan, N.; Thanasanvorakun, S.; Monajjemi, M. Investigation of single wall carbon nanotubes electrical properties and normal mode analysis: Dielectric effects. *Russian Journal of Physical Chemistry A* **2009**, *83*, 2288-2296, https://doi.org/10.1134/S0036024409130184.
42. Beak P., Covington J.B., Smith S.G., White J.M., and Zeiger J.M.,1980. Displacement of protomeric equilibriums by self-association: hydroxypyridine-pyridone and mercaptopyridine-thiopyridone isomer pairs . *J. Org. Chem* **1980**, 45, 1354-1362. https://doi.org/10.1021/jo01296a002.
43. Sarasia, E.M.; Afsharnezhad, S.; Honarparvar, B.; Mollaamin, F.; Monajjemi, M. Estrogenic active stilbene derivatives as anti-cancer agents: A DFT and QSAR study. *Phys. Chem. Liq.* **2011**, *49*, 561-571. https://doi.org/10.1080/00319101003698992.
44. Monajjemi, M.; Mahdavian, L.; Mollaamin, F.; Khaleghian, M. Interaction of Na, Mg, Al, Si with carbon nanotube (CNT): NMR and IR study. *Russ. J. Inorg. Chem* **2009**, *54*, 1465-1473. https://doi.org/10.1134/S0036023609090216.
45. Polzella, M.S.; Lodeyro, P. Re-evaluating semi-empirical computer simulations in quantum chemistry. *Found Chem* **2019**, *21*, 83-95. https://doi.org/10.1007/s10698-018-09329-w.
46. Kirkwood, J.G. On the Theory of Strong Electrolyte Solutions, *J. Chem. Phys* **1934**, *2*, 767. https://doi.org/10.1063/1.1749393.
47. Kirkwood, J.G. The Dielectric Polarization of Polar Liquids. *J. Chem. Phys* **1939**, *7*, 911. https://doi.org/10.1063/1.1750343.
48. Onsager, L. Electric Moments of Molecules in Liquids. *J. Am. Chem. Soc* **1936**, *58*, 1486-1493. https://doi.org/10.1021/ja01299a050.
49. Wong, M.A.; Frisch, M.J.; Wiberg, K.B. Solvent effects.1.The mediation of electrostatic effects by solvents, *J. Am. Chem. Soc* **1991**, *113*, 4776-4782. https://doi.org/10.1021/ja00013a010.
50. Zadeh, MAA.; Lari, H.; Kharghanian, L.; Balali, E.; Khadivi, R.; Yahyaei, H.; Mollaamin, F.; Monajjemi, M. Density Functional Theory Study and Anti-Cancer Properties of Shyshaq Plant: In View Point of Nano Biotechnology. *J Comput Theor Nanosci* 2015, *12*, 4358-4367. https://doi.org/10.1166/jctn.2015.4366.
51. Ghalandari, B.; Monajjemi, M.; Mollaamin, F. Theoretical Investigation of Carbon Nanotube Binding to DNA in View of Drug Delivery. *J.Comput.Theor.Nanosci* **2011**, *8*, 1212-1219, https://doi.org/10.1166/jctn.2011.1801.
52. 52.Monajjemi, M.; Farahani, N.; Mollaamin, F. Thermodynamic study of solvent effects on nanostructures: Phosphatidylserine and phosphatidylinositol membranes. *Phys. Chem. Liq* **2012**, 50, 161-172. https://doi.org/10.1080/00319104.2010.527842.